Article

Agates of the Lece Volcanic Complex (Serbia): Mineralogical and Geochemical Characteristics

Zoran Miladinović [1,*], Vladimir Simić [1], Nenad Nikolić [2], Nataša Jović Orsini [3] and Milena Rosić [3,*]

[1] Faculty of Mining and Geology, University of Belgrade, Đušina 7, 11000 Belgrade, Serbia; vladimir.simic@rgf.bg.ac.rs
[2] Institute for Multidisciplinary Research, University of Belgrade, Kneza Višeslava 1, 11030 Belgrade, Serbia; nnikolic@imsi.bg.ac.rs
[3] "Vinča" Institute of Nuclear Sciences, National Institute of the Republic of Serbia, University of Belgrade, Mike Petrovića Alasa 12-14, 11351 Belgrade, Serbia; natasaj@vin.bg.ac.rs
[*] Correspondence: zoran.miladinovic@rgf.bg.ac.rs (Z.M.); mrosic@vin.bg.ac.rs (M.R.)

Abstract: Agate veins and nodules occur in the Lece Volcanic Complex (Oligocene-Miocene) situated in the south of Serbia and occupying an area of 700 km^2. This volcanic complex is composed predominantly of andesites, with sporadic occurrences of andesite-basalts, dacites and latites, and features agate formations that have been very little investigated. This study focuses on five selected agate occurrences within the Lece Volcanic Complex, employing optical microscopy, scanning electron microscopy (SEM), X-ray powder diffraction analysis, inductively coupled plasma mass spectrometry (ICP-MS), and Fourier transform infrared spectroscopy (FTIR). In three localities (Rasovača, Mehane, and Ždraljevići), agate mineralization is directly related to distinct fault zones with strong local brecciation. In the other two localities (Vlasovo and Sokolov Vis), the agate is found in nodular form and does not show any connection with fracture zones. The silica phases of the Lece volcanic agates consist of cristobalite and tridymite, length-fast chalcedony, quartzine (length-slow chalcedony), and macrocrystalline quartz. Vein agates show a frequent alternation between length-fast chalcedony and quartz bands. Nodular agates consist primarily of length-fast chalcedony, occasionally containing notable quantities of opal-CT, absent in vein agates. Microtextures present in vein agates include crustiform, colloform, comb, mosaic, flamboyant, and pseudo-bladed. Jigsaw puzzle quartz microtexture supports the recrystallization of previously deposited silica in the form of opal or chalcedony from hydrothermal fluids. Growth lines in euhedral quartz (Bambauer quartz) point to agate formations in varying physicochemical conditions. These features indicate epithermal conditions during the formation of hydrothermal vein agates. Due to intense hydrothermal activity, vein agate host rocks are intensively silicified. Vein agates are also enriched with typical ore metallic elements (especially Pb, Co, As, Sb, and W), indicating genetic relation with the formation of polymetallic ore deposits of the Lece Volcanic Complex. In contrast, nodular agates have a higher content of major elements of host rocks (Al$_2$O$_3$, MgO, CaO, Na$_2$O, and K$_2$O), most probably mobilized from volcanic host rocks. Organic matter, present in both vein and nodular agate with filamentous forms found only in nodular agate, suggests formation in near-surface conditions.

Keywords: Lece Volcanic Complex; andesite; chalcedony; quartz; opal-CT; microtexture; organic matter

1. Introduction

Agate, a banded textural variety of chalcedony, may comprise other SiO$_2$ polymorphs and some paragenetic minerals such as calcite, clay minerals, and barite [1–3]. Agate is predominantly associated with volcanic host rocks such as basalt, andesite, and rhyolite, as well as tuffs, although it can also be found in sedimentary and metamorphic geological settings [4,5]. Based on the form of their occurrence, two basic types of agate can be

distinguished: (1) nodular (lithophysal or amygdaloidal) agate, formed by filling cavities produced by volatiles in lava, often termed volcanic agates, and (2) vein-type agate occupying veins and cracks in host rock [6].

Despite being utilized as a gemstone for several thousand years, its genesis is not fully explained. This is one of the factors that has hindered its artificial creation to date. Since agate is most often found in volcanic or surrounding rocks, its formation is most likely linked to volcanic activity [2–4,7].

The characteristics of agate in Serbia have not been thoroughly investigated due to the lack of tradition in its use, resulting in poor exploration of its occurrences. Most agate occurrences in Serbia were discovered during scarce geological explorations conducted in the 1980s by the state geological survey institutions such as Geozavod and Geoinstitute. Data from these investigations are primarily available in unpublished geological reports. An overview of the exploration results on agates and other gemstone occurrences is best presented by Ilić et al. [8]. However, numerous agate occurrences have been documented in the Jurassic ultramafics of Fruška Gora [9–11], Šumadija (Boblija [12,13] and Vučkovica [13,14]), and in the Tertiary volcanic complexes of Borač (quartz latite) [13,14] and Lece (andesitic) [13,15].

Rasovača agates were first mentioned by Cissarz et al. [16], and until 2012, it was the only known presence of agate in the Lece Volcanic Complex. The remaining four agate localities (Ždraljevići, Sokolov Vis, Mehane, and Vlasovo) were discovered by the first author of this paper during the research of the gemstone deposits of the Lece Volcanic Complex [17].

This study aims to investigate the mineralogical and geochemical characteristics of the Lece agates, highlighting the similarities and differences between different agate locations within the Lece Volcanic Complex, and providing data for understanding their genesis.

2. Geological Settings

The Tertiary Lece Volcanic Complex is an extremely important area in Serbia due to its abundant metal resources (Pb, Zn, Cu, Au, and Ag), which exhibit various types of geneses, and have long attracted the interest of many researchers. However, the geological studies of the volcanic rocks of the Lece complex have been limited. The most significant studies were conducted during the creation of the Basic Geological Map of SFR Yugoslavia, 1:100,000 [18–21], as well as the research conducted by Pešut [22,23].

The Lece Volcanic Complex is located in southern Serbia at the border between two large geotectonic units—the Serbian–Macedonian Massif and the Vardar Zone (Figure 1). The formation of this volcanic massif is heavily influenced by two regional fault structures. The first is the Tupale dislocation (Figure 1), extending over the eastern part of the Lece volcanic massif and continuing through the Tupale andesitic mass and further over the Bujanovac massif. The second regional fault structure is the Merdare dislocation, running along the western edge of the massif in the direction of Strezovce–Dražnja–Kravari–Kuršumlija (Figure 1).

These fault structures (Figure 1), intermittently active for an extended period, serve as crucial controlling factors for the volcanic processes and the subsequent formation of mineral deposits. The rocks of the Serbian–Macedonian Massif and Vardar Zone (Figure 1) underlying the Lece Volcanic Complex are characterized by complex geological history, significantly influencing the formation of specific structural features of the subsequently formed volcanic massif. According to Pešut [23], the basement rocks originated in connection with the deformations that most likely belong to the Variscian orogeny (Pz). During the period, spacious anticlinoria and synclinoria, nappe zones, dislocation zones with a series of fracture structures, and numerous smaller faults and cracks were created. The Lece Volcanic Complex formed along the existing fracture structures during the Alpine orogeny (Ol-M), [23]. After the main volcanic phases, new tectonic activity created extensive longitudinal and transverse fractures, enabling the formation of hydrothermal ore-bearing solutions [23].
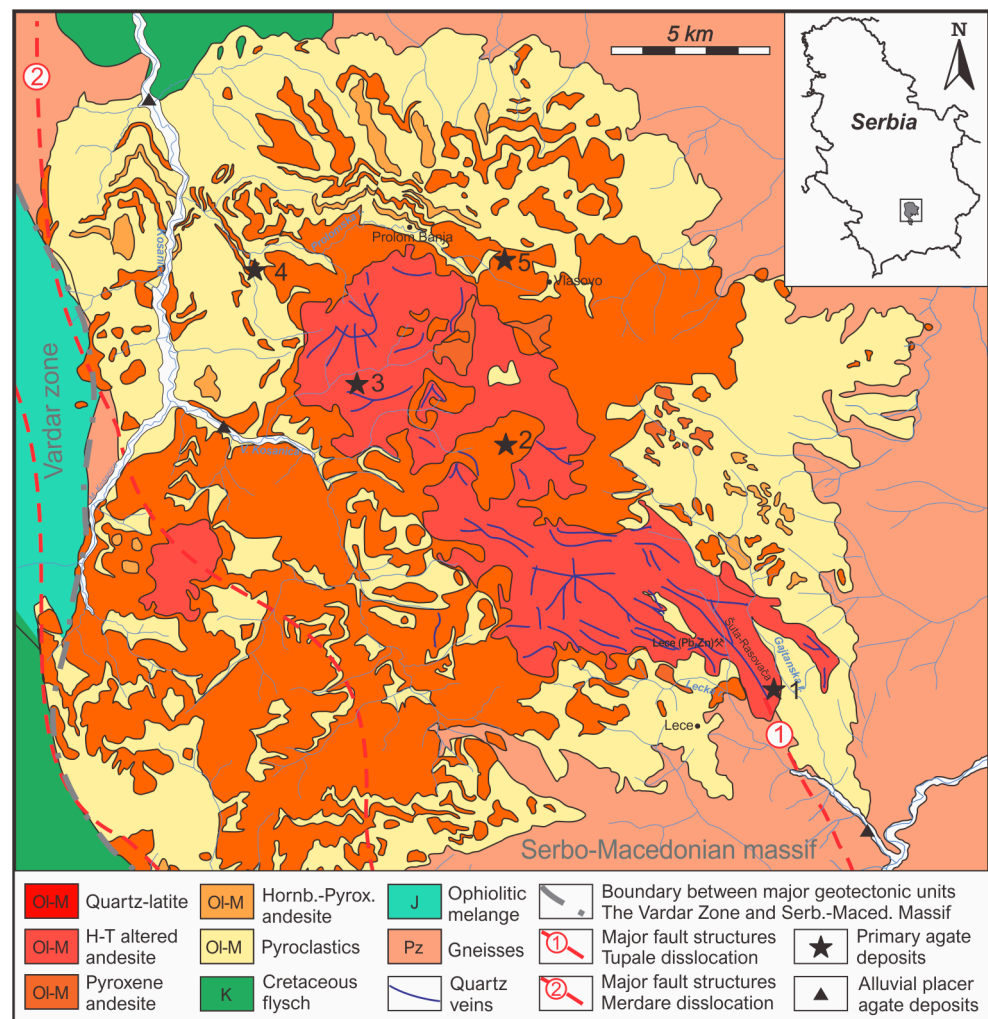
Figure 1. Simplified geological map of the Lece Volcanic Complex with locations of agate occurrences: 1. Rasovača, 2. Ždraljevići, 3. Sokolov Vis, 4. Mehane, 5. Vlasovo [18–21].

Based on stratigraphic studies, it is inferred that volcanic activity began in the Upper Oligocene and persisted during the Miocene [23]. According to scarce absolute dating investigations (K/Ar and U/Pb), the Lece volcanic rocks are 33.5 to 18 Ma old [24,25].

The Lece Volcanic Complex comprises two main groups of andesitic rocks: amphibole and pyroxene andesites. Apart from andesites and their pyroclastics, andesite basalts, dacites, and latites are also present to a much lesser extent. Andesites are predominantly found in the central parts of the Lece Volcanic Complex, while pyroclastics are more frequent in its peripheral parts. Amphibole andesites include hornblende andesites, hornblende-biotite andesites, hornblende-pyroxene andesites, hornblende-pyroxene andesites with biotite, and transitional types to dacites. The pyroxene andesites of the Lece Volcanic Complex include augite andesites, augite-hypersthene andesites, transition types to dacites, and andesite-basalts.

Pyroclastic rocks constitute approximately 40% of the volcanic complex and delineate the boundary between the volcanic rocks and the adjacent geological formations.

Pyroclastic rocks of the Lece Volcanic Complex manifest as volcanic breccias, volcanic agglomerates, and tuffs [23]. Volcanic agglomerates are less abundant than volcanic breccias and tuffs. The pyroclastic series attains a thickness of 100 m, with volcanic clasts ranging from one millimeter to over one meter. Hornblende andesite predominates in the composition of pyroclastic rocks, i.e., volcanic breccias and agglomerates. The mineral composition of tuffs comprises plagioclase, quartz, biotite, amphibole, and iron oxide

minerals. The minerals collectively form a fine-grained base with devitrified glass and sericite [23].

3. Agate Occurrences

Although the Lece Volcanic Complex has been intensively explored regarding metallic mineral resources, only one agate occurrence (Rasovača) was known before 2012 [17]. To date, five primary agate occurrences have been discovered, including Rasovača, Ždraljevići, Sokolov Vis, Mehane, and Vlasovo (Figure 1).

The Rasovača agate occurrence is located in the southeastern part of the Lece Volcanic Complex, approximately 1 km east of the Lece village, in the vicinity of the Lece polymetallic mine (Figure 1). Agates are found within the five-kilometer domain of intensely brecciated fault structure known as Šuta-Rasovača, with a general NNW-SSE trend. The polymetallic (Pb-Zn-Ag-Au) Lece deposit is related to the same zone. Both the deposit and the brecciated fault zone are situated in heavily hydrothermally altered andesitic and volcanoclastic rocks that reach several hundred meters in thickness. The intensity of hydrothermal alterations diminishes further away from the fracture zone. The agate occurrence lies in the southern segment of the fault zone at the Rasovača hill and extends approximately 1000 m along the zone. In addition to agate, amethyst and jasper also occur. Due to the repeated polyphase tectonic and hydrothermal activity, agate veins have been brecciated and cemented with an influx of new silica minerals (Figures 2A and 3A). In this location, agates occur mostly as breccia fragments. Agate veins are also present, but they are often brecciated. The size of agate clasts can reach up to approximately 30–40 cm. Deluvial placer accumulation on the slopes of Rasovača hill is rich in agate fragments. From both geological and economic points of view, Rasovača is one of the most significant gemstone occurrences in the Lece Volcanic Complex. The first utilization of agate probably dates back to the 6th century (CE), when it was utilized, alongside amethysts, in the fabrication of mosaics, as evidenced by the finds in the nearby early Byzantine archeological site of Iustiniana Prima [10].

The Ždraljevići agate occurrence lies in the central area of the Lece Volcanic Complex, 5 km to the south of the Prolom Banja spa, near the Ždraljevići hamlet. The occurrence is situated in intensely hydrothermally altered, silicified andesitic rocks along a fault zone measuring a few hundred meters in length and around 10 m in width. The thickness of the agate veins reaches thirty centimeters. Agate fragments can also be found on the slopes of the terrain. Lightly-colored amethyst bands can be frequently noticed in the agates found in Ždrljevići (Figure 2E).

The Sokolov Vis agate occurrence lies in the central area of the Lece Volcanic Complex, about 8 km to the south of the Prolom Banja Spa and approximately 2 km northwest of the geomorphological phenomenon known as Đavolja Varoš (Devil's Town) (Figure 1). The agate-bearing rocks were found near one of the highest peaks, Sokolov Vis, within the Lece Volcanic Complex, representing at the same time a prominent volcanic neck. Agates are found as small nodules in weathered hornblende andesite, with sizes ranging from 10 to 15 cm (Figure 2F). They are also present in the surrounding eluvial and deluvial placer accumulations.

The Mehane agate occurrence lies in the northern area of the Lece Volcanic Complex (Figure 1), 4 km west of Prolom Banja spa. The agates were identified in hornblende andesites and andesitic pyroclastics within a 30×250 m zone. Numerous agate veins were observed on the slope, particularly in the cut of a steep local mountain road. As altitude increases, the agate zone gradually transitions into weathered andesites. It is presumed that the agate occurrence may be significantly larger than the zone established so far, as agates have not been exploited in this area. Brecciation of the Mehane agates is less intense than in the Rasovača occurrence. Agate veins, somewhere over 50 cm wide, occasionally contain cavities filled with colorless and amethyst quartz crystals (Figure 2B,C).

Figure 2. Agate outcrops: (**A**)—Numerous fragments of agate and altered andesites cemented with silica minerals at the Rasovača occurrence; agate—(**A1**) and amethyst—(**A2**) fragments in tectonic breccia at the Rasovača occurrence. (**B**)—Outcrop of the agate vein in the Mehane occurrence with interesting black agate bands and brecciated agate fragments (where the tip of the pick hammer is pointing). (**C**)—Typical agate vein in the Mehane occurrence. (**D**)—Part of the agate nodule in the andesite at the Vlasovo occurrence. (**E**)—Small agate veins in intensely hydrothermally altered andesite at the Ždraljevići occurrence. (**F**)—Weathered andesites at the Sokolov Vis; (**F1**)—as a result of intense weathering digging out agates is easy; (**F2**)—agate nodules dug out from the weathered andesites at the Sokolov Vis occurrence.

The Vlasovo agate occurrence is located in the northern area of the Lece Volcanic Complex, in a quarry adjacent to the mountain road connecting Prolom Banja Spa to Vlasovo Village (Figure 1). The quarry covers an area of approximately 150 × 50 m. The host rocks are represented by relatively fresh hornblende with minimal hydrothermal alteration. A parallelepiped jointing of a part of the andesitic rock mass can be observed. Agates occur as nodules measuring up to 20 cm in size and as thin veinlets of up to 1–2 cm in thickness (Figure 2D).

In addition to the primary agate occurrences, significant amounts of agate have also been found in the secondary placer occurrences (Figure 1). Particularly interesting are alluvial placers of three rivers that run through the Lece Volcanic Complex: Velika Kosanica, Kosanica, and Lecka River [26].

Figure 3. (**A**)—Brecciated agate fragments cemented with red jasper from the Rasovača vein agate occurrence; (**B**)—Rasovača vein agate with healed fractures colored with iron oxide; (**C**)—two parts of wall lining vein agate from the Rasovača occurrence with predominantly yellow and white-colored bands and quartz filling the inner part; (**D**)—violet-blue colored vein agate from the Mehane occurrence; (**E**)—bluish-black vein agate with thin red bands from the Mehane occurrence; (**F**)—not completely filled vein agate with black and white agate bands in outer zone and bluish-greyish-white and red-colored bands in the inner zone from the Mehane occurrence; (**G**)—vein agate with amethyst bands from the Ždraljevići occurrence; (**H**)—the Sokolov Vis nodular agate with a black external zone and a greyish-white and red internal zone; (**I**)—wall-lining and horizontally layered (Urugay type)

agate from the Sokolov Vis occurrence; external wall lining zone is greyish-white and bluish with white and grey internal horizontally layered zone; (**J**)—nodular agate from the Sokolov Vis occurrence with a white external zone, a greyish-blue inner zone, and small quartz crystals in the open central part; (**K**)–nodular agate from the Vlasovo occurrence with a white outer zone and a greyish-blue and greyish-white inner zone, and a hollow center; (**L**)—bluish-white completely filled agate from the Vlasovo occurrence; (**M**)—red-brown-blue moss type agate from the Velika Kosanica river placer; (**N**)—nodular agate with a white outer zone, a red internal zone and small quartz crystals in the open central part from the Velika Kosanica river placer; (**O**)—yellowish-brown nodular agate from the Kosanica river placer.

4. Materials and Methods

Forty agate samples from all agate occurrences were cut, and twenty of them were polished (fifteen polished agate samples were selected and presented in Figure 3) for a better overview of agate textures. Petrographic analyses were conducted under the polarized microscope with transmitted light, and thin sections were made using Canada balsam.

Scanning electron microscopy was conducted at the Faculty of Mining and Geology of the University of Belgrade using a JEOL JSM–6610LV scanning electron microscope (SEM) coupled with an energy-dispersive X-Max Large Area Analytical Silicon Drifted spectrometer (Oxford, UK). The samples were coated with carbon using a sputter machine type BALTEC-SCD-005. The analyses were performed at an acceleration voltage of 20 kV, with a beam current of 20 nA and a spot size of 1 μm. A tungsten filament served as a beam source. Internal standards including Na–Albite, Al–Almandine, Si–Almandine, P–GaP, Cl–KCl, K MAD-10–Feldspar, Mn–Spessartine, Fe–Almandine, Zn–Zn, As–InAs, Sb–Sb, and Ba–BaF2 were used. The detection limit for most elements was ~0.1%.

Preliminary X-ray diffraction analysis and sample preparation were conducted at the Department of Petrology, Paleontology, and Mineralogy of the Geological Survey of Serbia. The analyses were performed employing a Philips PW-1710 automatic X-ray diffractometer (XRD). A long-focus copper anode (U = 40 kV and I = 30 mA) was used, with $K\alpha_1$ radiation (λ = 1.54060 Å) and a Xe proportional counter.

Additional X-ray diffraction analysis was performed on powdered samples of agates using a Rigaku SmartLab multipurpose X-ray diffractometer system in θ-θ geometry (the sample in horizontal position) in para-focusing Bragg–Brentano geometry at the "Vinča" Institute of Nuclear Sciences, National Institute of the Republic of Serbia, University of Belgrade. The system utilized a D/teX Ultra 250 strip detector in 1D XRF suppression mode with a Kβ-filtered CuKα1,2 radiation source (U = 40 kV and I = 30 mA). The XRD patterns were collected in a continuous scanning mode in a 2θ range of 5–70°, with a step of 0.01° and data collection speed of 0.4°/min. The mineral phase identification of the powder samples was performed in dedicated Rigaku PDXL 2.0 software with ICDD PDF-2 2016 database.

The FTIR spectra of the fine-grained powder materials from the agates were recorded using a Perkin Elmer Spectrum Two equipped with the Universal ATR accessory at the Institute for Multidisciplinary Research, University of Belgrade. The spectrum of each powder sample was recorded within the mid-infrared range of 4000–400 cm^{-1} with 20 scans and a spectral resolution of 4 cm^{-1}. Baseline correction and band position determination were performed using the Spectragryph software [27]. Band assignment was performed through comparison with reported data on analogous materials. The samples were prepared by pulverizing them in agate mortar. An incrustation in the geode was mechanically separated and ultrasonically treated in deionized water to force detachment of the incrustation matter. The resulting liquor was filtered through 2–3 μm pore size filter paper. Black residue was retained on the filter paper, while red residue was deposited from the filtrate. Both materials were analyzed by FTIR as separate samples.

Chemical analyses were conducted at Acme Analytical Laboratories, Vancouver, Canada. Specimens were previously ground to 100 mesh. The chemical analyses were performed using inductively coupled plasma mass spectrometry (ICP-MS) with the de-

termination of 41 trace elements, while the preparation was carried out with four acids attack. A 0.25 gr sample was heated to evaporation in three acids: HNO_3, $HClO_4$, and HF, followed by drying. The remaining residue was dissolved in HCl acid.

Inclusion analyses were performed using the Mueller optronic optical stereomicroscope with a magnification of up to $100\times$. The analyses were performed on polished agate samples observed in dark-field, transmitted, and reflected light.

5. Results

5.1. Macroscopic Observations

In the localities of Rasovača, Ždraljevići, and Mehane, agate mineralization occurs in the form of veins (Figure 3A–G), while in Vlasovo and Sokolov Vis, agates have a nodular shape (Figure 3H–L).

Vein agates exhibit differently colored bands ranging from colorless, white, grey, blue, brown, and brownish-yellow to red. Purple and black bands appear in Mehane agates. Amethyst often forms as a final product of crystallization in the center of the agate vein. Somewhere, voids are ultimately filled with brown jasper after the formation of euhedral quartz crystals (colorless or amethyst) (Figure 3E,F). Amethyst is particularly common in the Rasovača occurrence; this mineral, in addition to forming single bands of agate, occasionally forms druses with often closely intertwined crystals. Nodular agates are less colorful, especially those from the Vlasovo locality, which are mostly colorless grey with thin white and bluish bands. The Sokolov Vis agates exhibit a bit wider range of colors with brown, red, and yellow in addition to white, grey, and bluish bands.

Agates of the Lece Volcanic Complex are primarily of the wall-lining textural type, but water-level agates ("Uruguay type"—horizontally layered) occur in Sokolov Vis (Figure 3I). Moss agate varieties have also been found in the secondary placer occurrences (Figure 3M).

At the Rasovača agate occurrence, brecciated agates cemented with silica minerals (quartz, chalcedony, and jasper) are frequent (Figure 3A). The degree of brecciation is less intense at the Mehane and Ždraljevići agate occurrences.

In the nodular agates of the Sokolov Vis occurrence, quartz crystals occur in the central parts of the nodule, occasionally leaving an unfilled space after crystallization. Quartz crystals are almost absent in nodular agates from the Vlasovo locality.

Within vein agates, quartz, apart from the central parts of the agate veins, often builds agate bands (Figure 3). In addition to colorless quartz, amethyst occurs in all vein agate occurrences, but most frequently at the Rasovača occurrence. No amethyst has been found in the volcanic agates of Vlasovo and Sokolov Vis.

5.2. Optical Microscopy

5.2.1. Vein Agates

Length-fast chalcedony, along with macrocrystalline quartz, represents the most abundant silica phase in the Rasovača agates (Figure 4A,B). Quartzine (length-slow chalcedony) is much less abundant than length-fast chalcedony, but it occasionally forms thin agate bands. In the Rasovača agate, quartzine appears between quartz bands with subhedral quartz as a precursor and granular quartz as a successor (Figure 4A,B). A jigsaw-puzzle microtexture of quartz is also observed in the Rasovača agates (Figure 4I). Anhedral quartz crystals with irregular and interpenetrating boundaries (Figure 4I) are surrounded mainly with length-fast chalcedony, although quartzine and granular micro-quartz are also present. Small veinlets are often detected cross-cutting previously deposited silica minerals (Figure 4A).
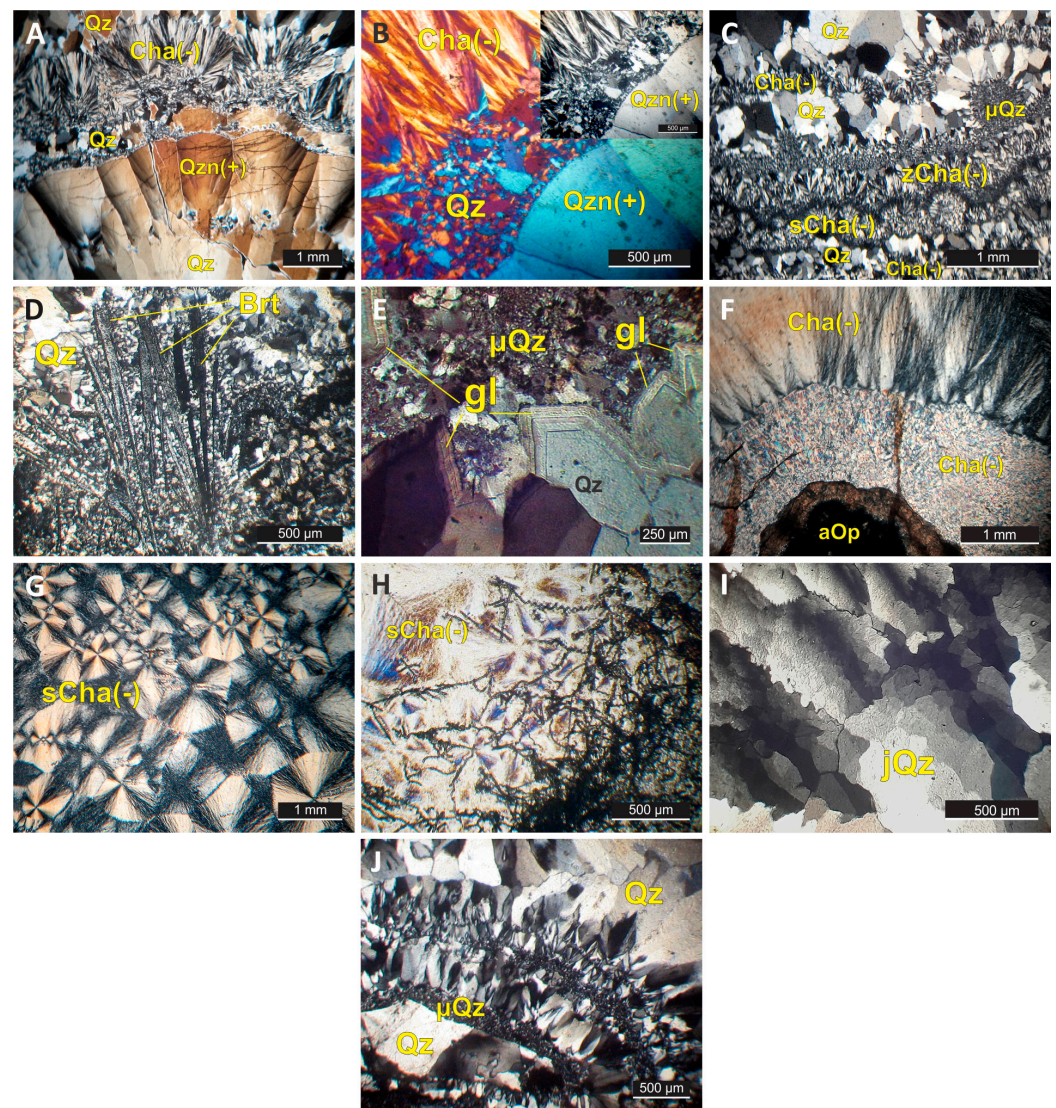
Figure 4. Photomicrographs of thin section agate samples. (**A**) Rasovača vein agate thin section with crossed polars (XP); frequent alteration of different silica phases—euhedral macroquartz crystals continue into length-slow chalcedony (quartzine), followed by a thin layer of macroquartz, length-fast chalcedony and macroquartz. (**B**) The same thin section as the previous photo (**A**)—crossed polars with λ-compensator; quartzine layer turning into macroquartz followed by length-fast chalcedony; right upper corner same photo without λ-compensator. (**C**) Mehane vein agate thin section (XP); frequent alteration of thin quartz and chalcedony bands; in 2.5 mm range, eight separate quartz and chalcedony layers. (**D**) Mehane vein agate thin section (XP); barite laths surrounded with quartz. (**E**) Mehane vein agate thin section (XP); growth lines in euhedral quartz crystals (Bambauer quartz). (**F**) Sokolov Vis nodular agate thin section (XP); presence of opal in the peripheral part of agate nodule succeeded with length-slow chalcedony layers. (**G**) Vlasovo nodular agate thin section (XP); spherulitic chalcedony. (**H**) Vlasovo nodular agate this section with parallel polars (PP); the same thin section as in the previous photo (G); filamentous forms embedded in spherulitic chalcedony. (**I**) Rasovača vein agate thin section (XP); mosaic quartz with interpenetrating boundaries (jigsaw puzzle quartz). (**J**) Ždraljevići vein agate thin section (XP); agate bands dominantly made from quartz. Abbreviations: Qz—macrocrystalline quartz, μQz—microcrystalline quartz, Cha(-)—length-fast chalcedony, zCha(-)—zebraic chalcedony, Qzn(+)—length-slow chalcedony (quartzine), aOp—amorphous opal, sCha(-)—spherulitic chalcedony, jQz—mosaic quartz (jigsaw puzzle quartz), gl—growth lines of Bambauer quartz, Brt—barite.

The Mehane agate is distinguished by the frequent alternation of chalcedony and quartz layers. These agates are rich in barite crystals (Figure 4D), but are often replaced with quartz (quartz pseudomorph after barite). Although less common, black and violet agate bands also occur. The red color is often attributed to hematite inclusions (Figure 5B).

Chalcedony is typically present as length-fast, occasionally forming a spherical and zebraic microtextural variety (Figure 4C). Quartz occurs as macrocrystalline quartz with crystals being anhedral and euhedral. Granular microquartz occurs frequently (Figure 4C). Jigsaw puzzle quartz microtexture is also present. Anhedral crystals often appear in the form of jigsaw puzzle quartz (Figure 4I).

Petrographic analysis of the Ždraljevići agate thin sections revealed that agate veins are predominantly made of macrocrystalline quartz (Figure 4J), with chalcedony appearing only sporadically. Abundant quartz occurs in the form of granular microquartz, jigsaw-puzzle quartz, and prismatic anhedral macroquartz crystals. Fe-oxide minerals occur as irregularly shaped inclusions between quartz grains and as small cross-cutting veinlets.

Euhedral quartz crystals with lamellar growth lines were observed in the Mehane and Rasovača agates (Figure 4E). Such microtextural features, also known as Bambauer quartz [28], are common in epithermal hydrothermal vein agates.
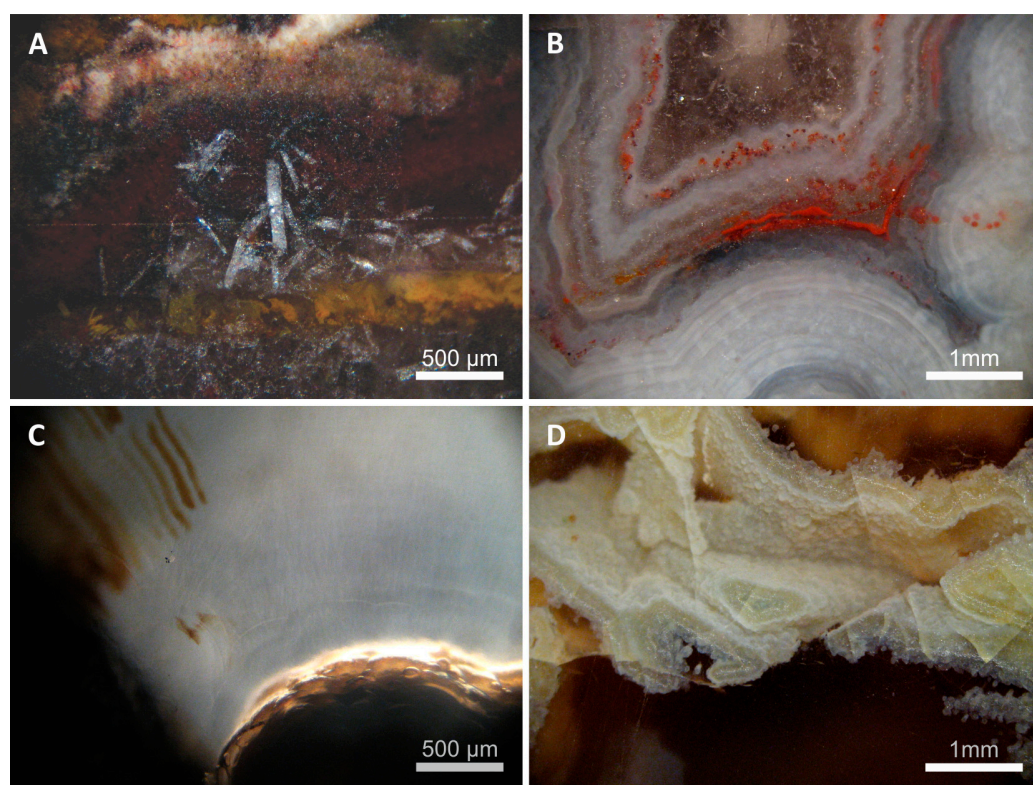

Figure 5. Photomicrographs of agate inclusions seen under gemological microscope. (**A**)—White tabular barite and light brown Fe-oxide inclusions in the Mehane vein agate (reflected light); (**B**)—Fe-oxide inclusions in the Mehane vein agate (reflected light). (**C**)—Fe-oxide inclusions in the Sokolov Vis agate (dark field illumination) with spherulitic chalcedony aggregates as nucleation centers (down right); (**D**)—small flaky quartz pseudomorphs after calcite (?) in Sokolov Vis agate (reflected light).

5.2.2. Nodular Agates

Petrographic investigations of nodular agates from two localities (Vlasovo and Sokolov Vis) indicate that their silica matrix is mainly made of chalcedony, with macro-crystalline quartz present in smaller quantities. Chalcedony is predominantly length-fast, with spherulitic chalcedony also being observed.

In the nodular agates, macrocrystalline quartz is less abundant compared to vein agates. There is no macrocrystalline quartz in the banded zones of nodular agates of Vlasovo and Sokolov Vis. Quartz is usually formed in the center of the agate nodule as the final silica phase (Figures 4 and 5). Occasionally, macroquartz is entirely absent in nodular agates.

Interesting filamentous forms are embedded in the spherulitic chalcedony of the Vlasovo agate (Figure 4G–H). These curious forms are similar to the ones found in the Hungarian agates from the Matra Mts andesites [3]. However, macroscopically, the Matra Mts and Vlasovo agates exhibit significant differences. Matra agates are highly colorful, while those from Vlasovo lack such vivid colors (Figure 3K,L).

The Sokolov Vis agates are predominantly composed of length-fast chalcedony, with macrocrystalline quartz occurring in the central portion of nodules (Figure 3H,J). At the periphery of the agate geode, at the contact with the host rock, opal is observed, followed by granular and fibrous chalcedony (Figure 4F). Iron oxide inclusions contribute to the coloring of agate bands (Figure 5A–C). Pseudomorphism is present in some specimens where flaky quartz replaces previously formed crystals, probably calcite (Figure 5D).

5.3. Scanning Electron Microscopy (SEM)

SEM analyses revealed different inclusions in the silica matrix. It has been noticed that the use of cathodoluminescent imaging facilitates the distinction between separate silica phases (Figure 6). The most prevalent inclusions, especially in the Rasovača and Mehane vein agates, are iron oxide (Figure 6A). Titanium and manganese oxide inclusions were also detected at the Mehane agate occurrence. Numerous euhedral barite crystals in the Mehane agate are often completely replaced with silica (Figure 6A), making their identification difficult. Barite crystals typically occur in an agate band made of quartz. Euhedral quartz crystals usually occupy the central part of agate veins.
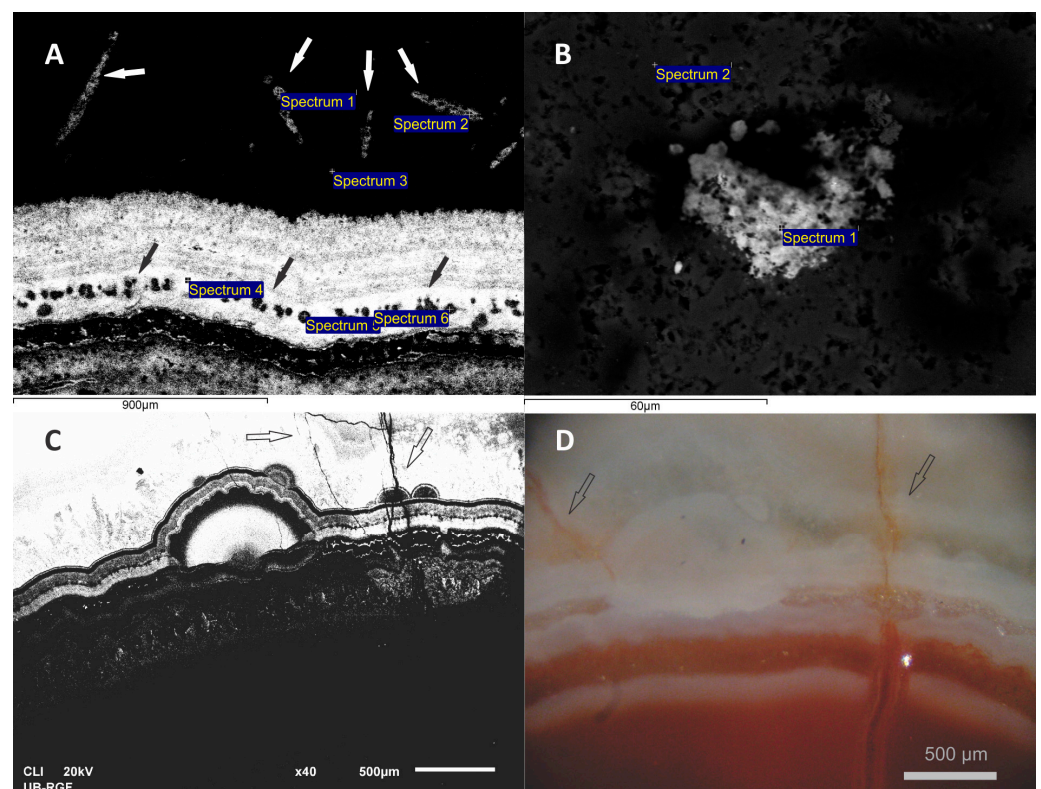

Figure 6. SEM micrographs of the Mehane (**A**,**B**) and the Rasovača (**C**,**D**) vein agate samples. (**A**) Micrograph (CLI SEM) of Mehane vein agate showing barite inclusions (white arrows) and Fe-oxide inclusions (black arrows) concentrated within the agate band. The barite crystals are largely

replaced by silica and are therefore hardly detectable in chemical analyses (Table 1). (**B**) Fe-oxide inclusions in the SE (secondary electron) (chemical analyses in Table 1). (**C**) Microscopic image (SEM CLI) of the agate sample from the Rasovača occurrence in conjunction with a photomicrograph of a similar area (**D**) taken under the gemological microscope in transmitted light (right). Multiphase hydrothermal activity is demonstrated by silica veinlets (arrows) that cross-cut previously formed agate bands.

Table 1. Chemical analyses corresponding to the SEM micrographs shown in Figure 6A,B.

	Figure 6A			**Figure 6B**	
	Formula	Wt%		Formula	Wt%
Spectrum 1	Na_2O	0.27	Spectrum 1	Na_2O	0.77
	SiO_2	99.73		Al_2O_3	1.07
Spectrum 2	SiO_2	100		SiO_2	2.31
Spectrum 3	SiO_2	100		P_2O_5	1.07
Spectrum 4	SiO_2	100		K_2O	0.2
Spectrum 5	SiO_2	100		Fe_2O_3	93.38
Spectrum 6	Na_2O	0.41		As_2O_3	0.79
	SiO_2	99.35		BaO	0.41
			Spectrum 2	SiO_2	100

5.4. XRD Analysis

The X-ray powder diffraction was performed to determine the silica phase composition and the presence of other minerals. Seven agate samples underwent XRD analyses.

Vein agate samples: Mehane–LMII4, Ždraljevići: LZ2.

Nodular agate samples: Vlasovo: LPV2, LPV3; Sokolov Vis: LMDJ2, LSV2, LSV3.

The dominant silica phase detected is α quartz, and the narrow width of reflections indicates high quartz crystallinity (Figure 7). Opal-CT is observed in the agate specimens from the Vlasovo and Sokolov Vis localities.

The complex reflection ranging from 4.11–4.04 Å (21.6–21.95 2 theta), characteristic of opal-CT, is observed only in the nodular agate samples (LPV-2, LPV-3, LSV-2, LSV-3) (Figure 8). The intensity of opal-CT reflections is much higher in the LPV-2 sample compared to the other nodular samples. The position of reflection maxima varies across the nodular sample suite, spanning from 4.04 to almost 4.11 (Figure 8). In extension of previously published work by Jones and Segnit [29], Ghisoli et al. [30] conducted an XRD study of 75 opal samples worldwide and proposed a simple classification of opal-CT based on the position of diffraction maxima within the range of 4.11–4.04 Å, spanning from theoretical tridymite (4.11 Å) to cristobalite (4.04 Å) in a cristobalite-tridymite stacking sequence. Therefore, all nodular opals examined in this study could be classified as opal-CT with varying amounts of cristobalite and tridymite. While LPV-3 opal predominantly comprises opal-C (4.04 Å), LSV-2 is more tridymite-rich in a cristobalite-tridymite stacking sequence (4.11–4.08 Å broad reflection). The degree of disorder in the cristobalite-tridymite superstructure is reflected in the broadening of the diffraction maxima. Earlier research by Flörke [31] and more recently by Ghisoli et al. [30] argued for an increase in disorder in the opal-CT structure with the rise in the α-tridymite band in the XRD patterns. This increase in disorder is evident in the conspicuous reflection broadening observed in LSV-2, nearing 4.11 Å (Figure 8). Such broadening, indicating a predominance of noncrystalline matter, resembles a pattern of noncrystalline opal-A, which is more consistent with the "paracrystalline model" for opal-CT proposed by Smith [32], with latter contributions [33] for tridymite-rich opal end member.
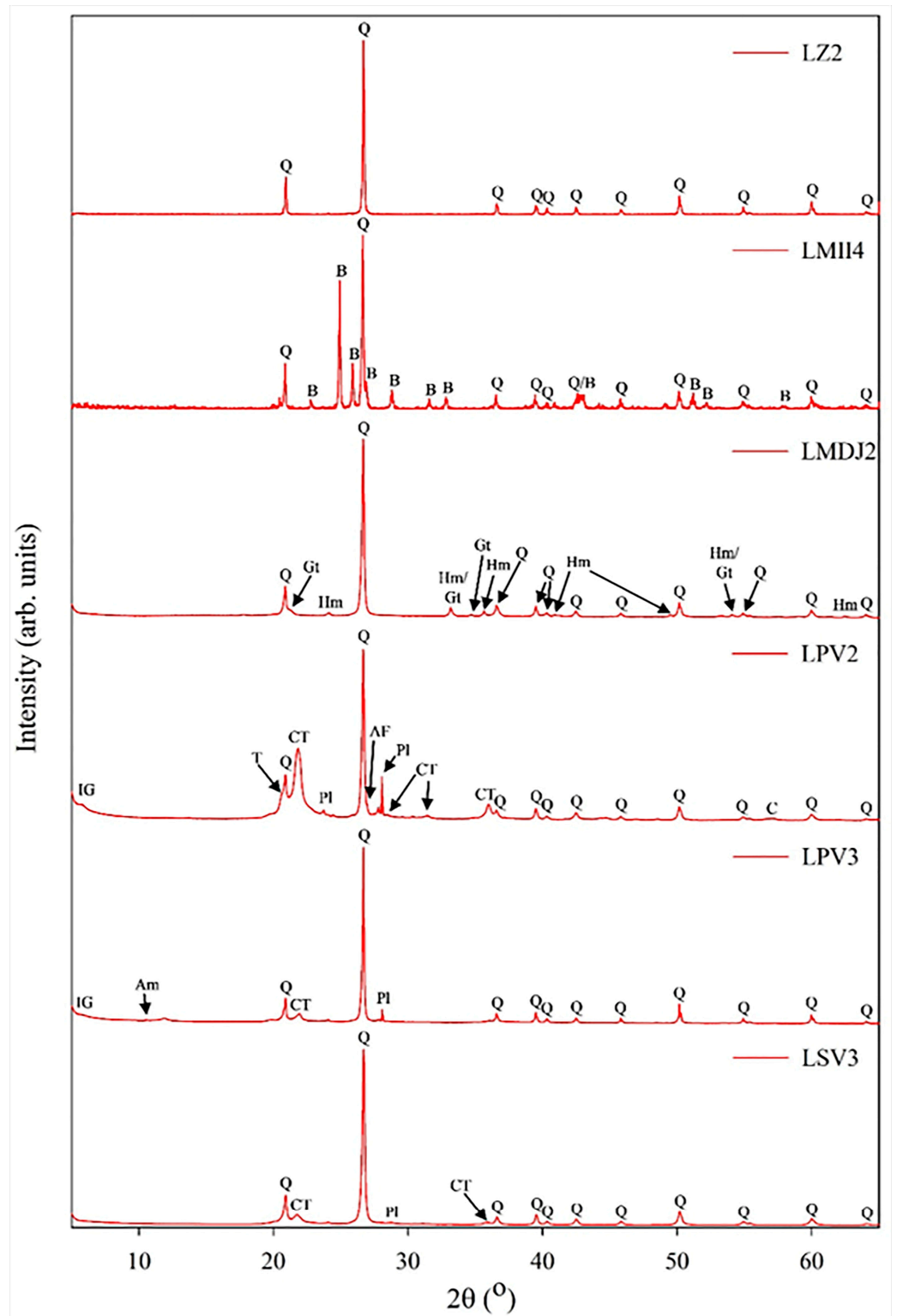
Figure 7. XRD pattern of agate samples from the Lece Volcanic Complex. LZ2 and LMII4 are veined agates while the others are nodular agates. Abbreviations: Q—quartz, IG—interstratified clay, CT—opal-CT, B—barite, Hm—hematite, Gt—goethite, Pl—plagioclase, AF—alkali feldspar, Am—amphibole.
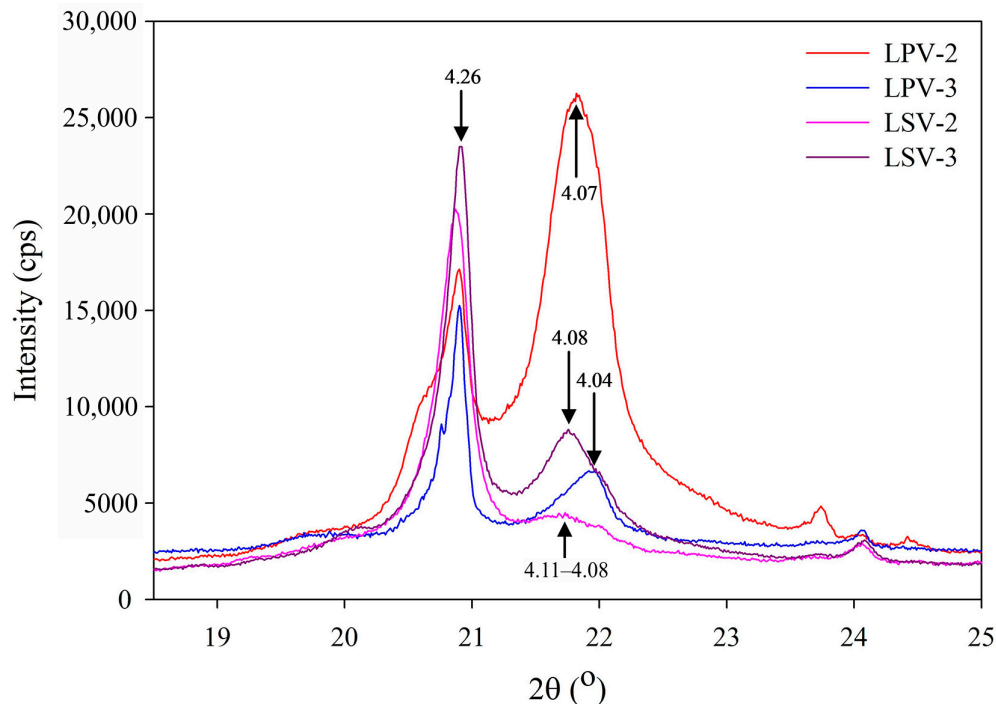
Figure 8. XRD pattern of nodular agate samples from the Lece Volcanic Complex. The complex reflection consists of 4.26 Å pertaining to quartz and CT-opal reflection in the range of 4.11–4.04 Å. Agate samples reveal a shift in the opal reflection position indicating variation of α-cristobalite and α-tridymite portion in the opal stacking sequence.

In addition to the prevalent quartz, the high-intensity reflections of barite, such as 3.57 Å (200), 3.44 Å (021), and 3.32 Å (210), are identified only in vein agate samples from the Mehane occurrence (LMII-4) (Figure 7), indicating a significant quantity of barite, which is consistent with FTIR and optical microscopy observations. The low-intensity reflections pertaining to plagioclase feldspar, specifically 3.178 Å (002) and 3.208 Å (040), are observed in nodular opal samples LPV-2 and LPV-3, while barely observable in LSV-3 and veined agate LMII-2 (Figure 7). They correspond to a disordered intermediate plagioclase composition. The smallest amount of alkali feldspar (peaks at 3.304 Å) is observed only in the LPV-2 nodular sample, manifesting as a weak shoulder on the more intense quartz reflection (Figure 7). Hematite and goethite are only observed in the LMDJ-2 sample, which is consistent with its distinct red color and microscopic observations. (Figure 7). The weak and broad reflection at approximately 15–16 Å observed in nodular LPV-2 and LPV-3 is attributed to interstratified clay.

5.5. FTIR Analysis

Nine agate samples were subjected to FTIR analyses.
Vein agate samples: Rasovača–LR2; Mehane–LMI2, LMII2, LMII3; Ždraljevići: LZ2.
Nodular agate samples: Vlasovo: LPV2, LPV3; Sokolov Vis: LSV2, LSV3.

The component identification based on characteristic band vibrations, providing information on functional groups in the fingerprint region of 1800–400 cm^{-1}, is shown in the right pane of Figure 9, while the OH-region falling in the 3800–2600 cm^{-1} range is shown in the left pane.

Very weak bands at 3750 and 3737 cm^{-1} are observed in all samples, except in LZ-2 and the rock crystal referent quartz sample spectrum (Figure 9). The 3737 cm^{-1} band displays asymmetry towards lower wavenumbers. They are attributed to stretching vibrations of silanol (SiOH) groups: isolated silanol (free OH) in the former and hydrogen-bonded silanol in the latter [34–36].
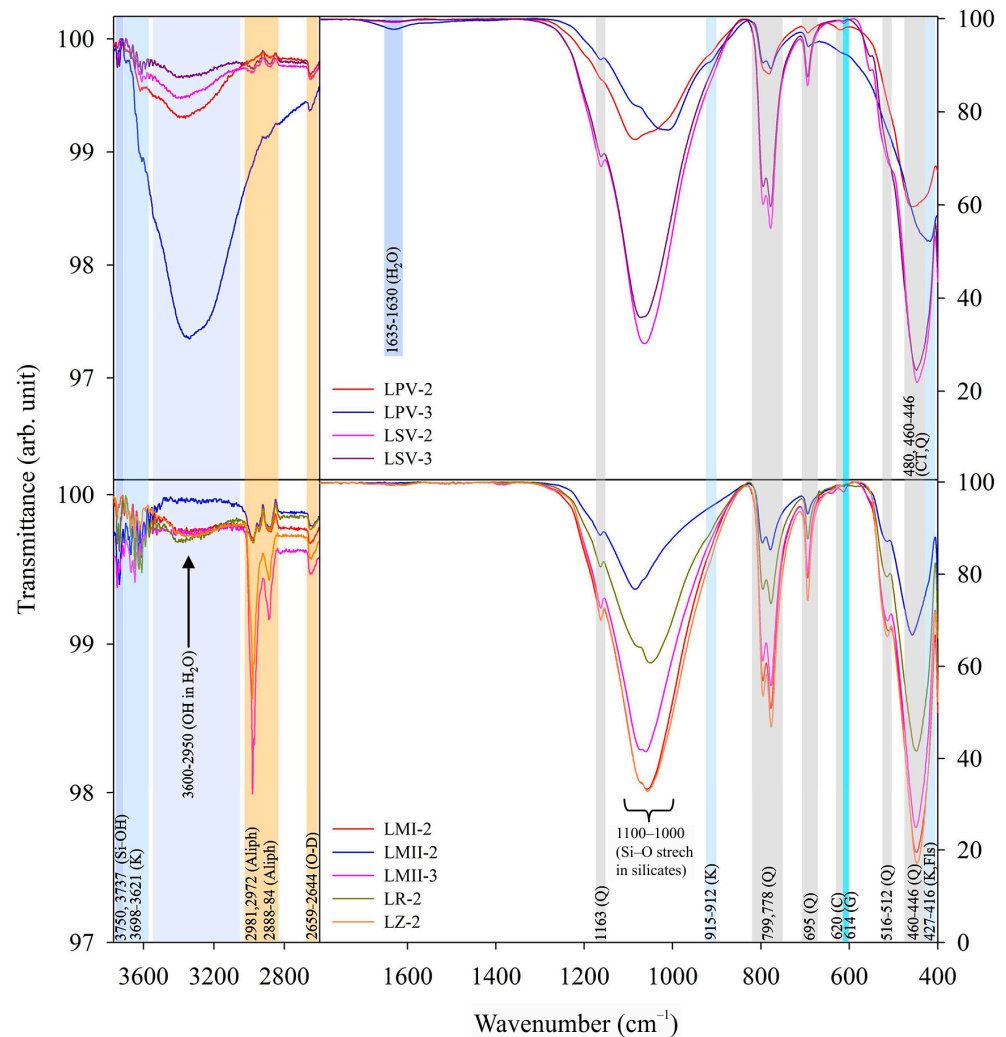
Figure 9. FTIR spectra of agate samples from the Lece Volcanic Complex. The OH-region and aliphatic organic component regions (3800–2600 cm^{-1}) are shown in the left pane, while the fingerprint region (1800–400 cm^{-1}) is shown in the right pane. Abbreviations: Q—quartz, K—kaolinite, G—goethite, Fls—feldspar, CT—opal, C—cristobalite, Aliph—aliphatic component.

Opal-CT present in nodular agate samples (LPV-2, LPV-3, LSV-2, LSV-3) displays a broad featureless band in the 3600–2950 cm^{-1} OH-region. A more intense band, indicating higher water content, is recorded in LPV-3. In contrast, vein agate samples (LMI-2, LMII-2, LMII-3, LMII-4, LR-2, LZ-2) do not show any features in the OH-region. However, this anhydrous sample suite is characterized by a doublet at 2981 and 2972 cm^{-1}, which is relatively more intense compared to the weak and barely observable ones in the nodular agate suite. These modes are assigned to C-H symmetric and asymmetric stretching vibrations in –CH$_2$ and –CH$_3$ groups [37]. A weak broad band in the range of 2888–2884 cm^{-1} is also observed in the anhydrous sample suite, while being well resolved in LMII-3 and LZ-2 compared to the others. In the nodular agate suite, this band is barely observable and is assigned to C-H symmetric stretching vibrations in the alkyl group (–CH$_2$) [38].

The LPV-3 sample represents the black-colored matter lining the cavity; essentially, it is an incrustation in the geode of the nodular agate LPV-2 sample. Compositionally, LPV-3 is a mixture predominantly comprising quartz and opal-CT, as inferred from XRD-FTIR analyses (Figures 7 and 9). After being ultrasonicated and filtered, this incrustation material, separated as a black matter on filter paper, shows a very similar pattern to LPV-3, only with a higher water content inferred from more intense bands in the OH-region and H$_2$O bending region (black residue in Figure 10). However, the red-colored suspension deposited

from the filtrate reveals a distinct FTIR spectrum (red residue in Figure 10). In addition to a much higher water content inferred from the OH stretching and H_2O banding regions, in the aliphatic region, the resolved doublet at 2969–2960 cm^{-1} and 2954 cm^{-1} is assigned to methyl groups attached to alkyl chains and aromatic rings [39], and 2933–2927 cm^{-1} and 2854 cm^{-1} to –CH$_2$ asymmetric and symmetric stretching [40], respectively. The prominent broad bands in the fingerprint region of this LPV-3 red suspension (red residue) at 1591, 1468, 1412, 1365, and 1321 cm^{-1} are assigned to C=C aromatic in-plane skeletal, C–H deformation combined with aromatic ring, C-H banding, CH$_2$ banding, and CH in-plane banding vibrations, respectively (e.g., [41–44]).
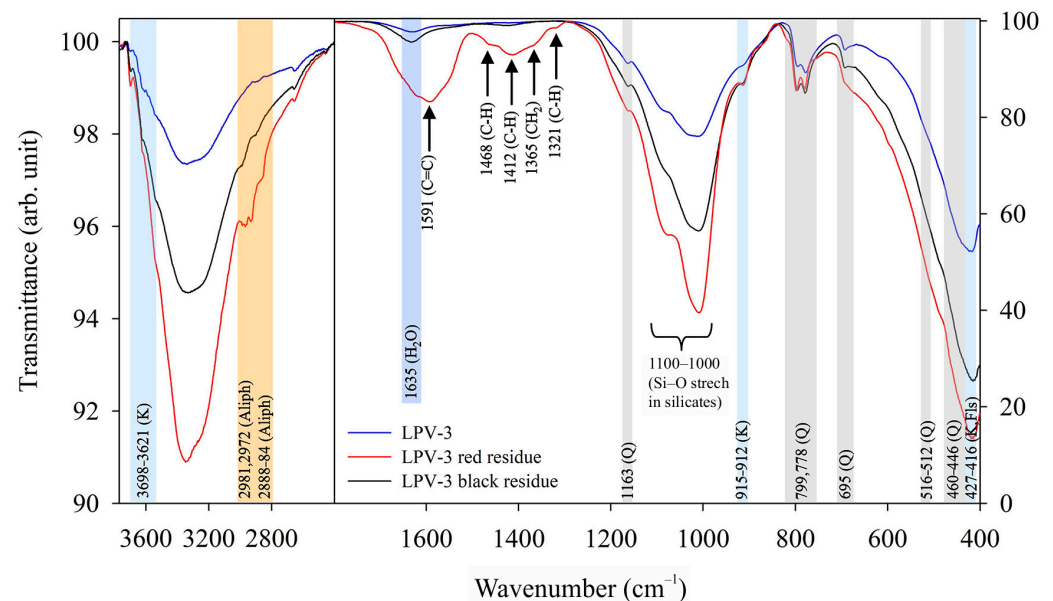

Figure 10. FTIR spectra of LPV-3 nodular agate and the incrustation lining cavity in geode from the Lece Volcanic Complex. Red and black residues are attributed to incrustation (explained in text). The left pane illustrates the OH-region and aliphatic organic component regions (3800–2600 cm^{-1}, while the right pane displays the fingerprint region of (1800–400 cm^{-1}). Abbreviations: Q—quartz, K—kaolinite, Fls—feldspar, Aliph—aliphatic component.

In the fingerprint region of 1900–400 cm^{-1}, the most intense broad complex band in the 1030–1000 cm^{-1} range is assigned to the in-plane Si–O–Si stretching vibration in silicates. The most prominent band at *ca* 464 cm^{-1} followed by bands at *ca* 1163, 1086 (shoulder), a doublet at 799 and 778, and 695 cm^{-1} are assigned to v4(Si–O) asymmetrical banding, v3(Si–O) asymmetrical stretching, v1(Si–O) symmetrical stretching, and v2(Si–O) symmetrical banding in quartz. Quartz, as the most dominant component, is determined in all examined samples. The 695 cm^{-1} symmetrical banding vibration, related to octahedral site symmetry and serving as a diagnostic indicator of the crystallinity of quartz, appears relatively intense and sharp in all samples except for LPV-2, indicating a somewhat lower degree of crystallinity in the latter.

Weak bands observed at 983, 634, and 609 cm^{-1} in LMII-4 (vein agate sample), indicating the presence of sulfates, are assigned to v1(SO$_4^{2-}$) symmetrical stretching and for the last two v4(SO$_4^{2-}$) out-of-plane banding vibrations of sulfate group [45,46]. These band positions strongly correspond to baryte, which is consistent with XRD findings. Other strong bands, approximately at 1170 and 1070–1060 cm^{-1}, expected to be observed in baryte, strongly overlap with strong bands of the more abundant quartz.

The presence of a very weak band in LSV-2 at 614 cm^{-1} is assigned to Fe–O stretching of goethite [47,48]; other strong bands (e.g., 798 cm^{-1}) in goethite overlap with those of quartz. Hematite bands, although identified by XRD, were not observed due to overlap with quartz bands.

In the nodular agate suite, a strong absorption band at 620 cm^{-1}, reported as a diagnostic absorption band of α-cristobalite, is only observed in LPV-2 and not in the other samples (LPV-3, LSV-2, LSV-3) (Figure 9). Wilson [33] argued for the absence of this band in opal-CT in several studies, suggesting the spectra similar to those of tridymite and silica glass. Other opal bands strongly overlap those of quartz, except for a shoulder at *cca* 480 cm^{-1} recorded in LPV-3, occurring between the cristobalite band at 483 cm^{-1} and the tridymite band at 478 cm^{-1}, as reported by Chukanov [49].

5.6. ICP-MS Analysis

ICP-MS trace elements analyses were carried out on three agate samples and three host rock samples from three different occurrences: Mehane, Ždraljevići, and Vlasovo.

The host rocks in Mehane and Ždraljevići have been altered by hydrothermal solutions, resulting in a reduced weight percentage of some major elements of the host rocks (MgO, CaO, and Na$_2$O) due to the high degree of silicification. Furthermore, the host rocks are enriched with ore elements, such as Pb, Zn, Cu, As, and Sb, due to their hydrothermal activity. In contrast, the Vlasovo agate host rock is less altered and not so enriched with the abovementioned ore elements compared to the Mehane and Ždraljevići locations (Table 2). However, some elements, such as Ni, Co, V, Cr, and Mn, display higher contents in the Vlasovo host rock because it is less altered (silicified) and reveals the typical geochemistry of Meso-Cenozoik andesite [50]. Similarly, the values of Zr, Y, and Nb in the Vlasovo host rock are higher due to the lower alteration degree of the andesite host rock.

Table 2. The results of ICP-MS analysis of agate and host rock samples.

Sample	LPV-2	LMII-3	LZ-2	LPV-1	LMII-1	LZ-1	
	Nodular	**Vein Agate**			**Host Rocks**		
Local.	Vlas.	Meh.	Ždralj.	Vlas.	Meh.	Ždralj.	
(wt.%)							DL
Al$_2$O$_3$	2.66	0.17	0.95	14.18	13.40	13.83	0.01
TiO$_2$	0.105	0.007	0.023	0.695	0.396	0.434	0.001
FeO	2.77	0.73	0.60	5.72	4.16	5.86	0.01
MgO	0.68	0.02	0.05	3.22	0.38	0.73	0.01
CaO	0.71	0.04	0.08	6.82	0.49	0.13	0.01
Na$_2$O	0.377	0.012	0.041	3.609	0.644	0.081	0.001
K$_2$O	0.24	0.04	0.08	1.27	4.92	2.09	0.01
P$_2$O$_5$	0.032	0.002	0.016	0.238	0.108	0.224	0.001
S	<0.1	<0.1	<0.1	<0.1	<0.1	0.2	0.1
Total	7.59	1.02	1.84	35.75	24.50	23.38	
(ppm)							
Mo	2.0	0.4	0.4	0.9	0.8	5.7	0.1
Cu	32.4	8.2	41.1	47.2	14.3	337.6	0.1
Pb	15.8	101.6	348.4	31.9	25.0	6585.8	0.1
Zn	33	60	32	74	80	294	1
Ag	0.3	2.7	1.8	0.2	0.5	1.9	0.1
Ni	34.8	23.3	41.7	42.8	11.7	6.6	0.1
Co	7.4	132.0	183.0	31.8	25.1	1.7	0.2
Mn	7082	801	46	863	401	166	1
As	12	358	20	6	59	32	1
U	1.2	1.1	0.3	3.1	2.9	3.0	0.1
Au	<0.1	<0.1	<0.1	<0.1	<0.1	<0.1	0.1
Th	2.1	0.1	0.8	10.4	14.6	11.0	0.1
Sr	126	145	20	674	287	178	1
Cd	0.2	<0.1	<0.1	0.2	<0.1	0.7	0.1
Sb	26.8	322.1	39.1	1.2	103.2	16.4	0.1
Bi	0.3	0.1	4.0	0.1	<0.1	3.0	0.1
V	37	10	3	140	78	77	1

Table 2. *Cont.*

Sample	LPV-2	LMII-3	LZ-2	LPV-1	LMII-1	LZ-1	
	Nodular	Vein Agate		Host Rocks			
Local.	Vlas.	Meh.	Ždralj.	Vlas.	Meh.	Ždralj.	
Cr	33	3	4	88	15	16	1
Ba	1416	4006	55	828	2253	618	1
W	0.6	>200.0	192.4	126.3	183.8	4.0	0.1
Zr	17.8	0.2	2.9	119.6	74.1	27.0	0.1
Sn	2.1	<0.1	0.3	1.5	0.7	4.4	0.1
Y	7.0	0.9	1.2	15.0	12.0	4.3	0.1
Nb	1.9	<0.1	<0.1	12.8	4.0	5.3	0.1
Ta	0.1	<0.1	<0.1	1.2	0.8	0.4	0.1
Be	2	3	<1	2	1	2	1
Sc	3	<1	<1	17	10	11	1
Li	6.1	6.2	52.2	9.9	28.1	16.0	0.1
Rb	13.7	0.9	3.4	17.2	242.2	89.5	0.1
Hf	0.4	<0.1	<0.1	3.1	2.1	0.8	0.1
La	7.8	1.4	2.8	22.2	25.4	15.6	0.1
Ce	14	3	5	45	41	32	1

The discovery of the Ždraljevići agates was facilitated by the field geological work (trenching) conducted during the investigation of polymetallic mineralization, as they practically make an integral part of that ore occurrence.

The major element contents in vein agates (Mehane and Ždraljevići) differ from nodular agates from Vlasovo. There are significantly higher concentrations of Al_2O_3, MgO, CaO, Na_2O, and K_2O in the Vlasovo agate compared to those from Mehane and Ždraljevići (Figures 11A and 12).
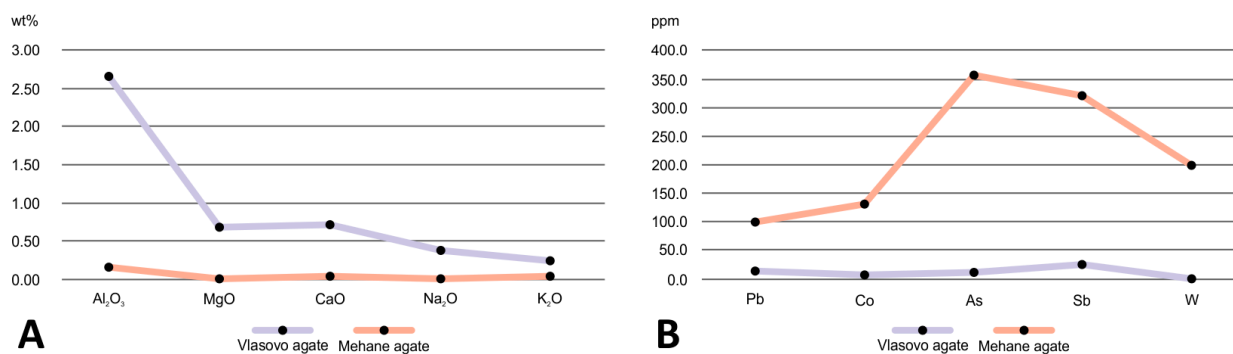

Figure 11. Major elements (**A**) and ore elements (**B**) in the Vlasovo nodular agate (LPV-2) and the Mehane vein agate (LMII-3).

On the other hand, there is an evident increase in ore elements in vein agates (Mehane and Ždraljevići) compared to nodular ones (Vlasovo). In addition to the anticipated higher amounts of Pb, Zn, and Cu due to numerous polymetallic occurrences and deposits in the Lece Volcanic Complex, there are also significantly increased contents of Co, As, Sb, and W (Figure 11B).

The contents of Rare Earth Elements (Y, Sc, La, and Ce) are elevated in the Vlasovo agates compared to those in vein agates. The highly increased Ba content in the Mehane vein agate aligns with the results of XRD, SEM, and petrographic analyses confirming the presence of barium. There is a clear difference in trace element contents between vein agates (Mehane and Ždraljevići) and nodular agates (Vlasovo).
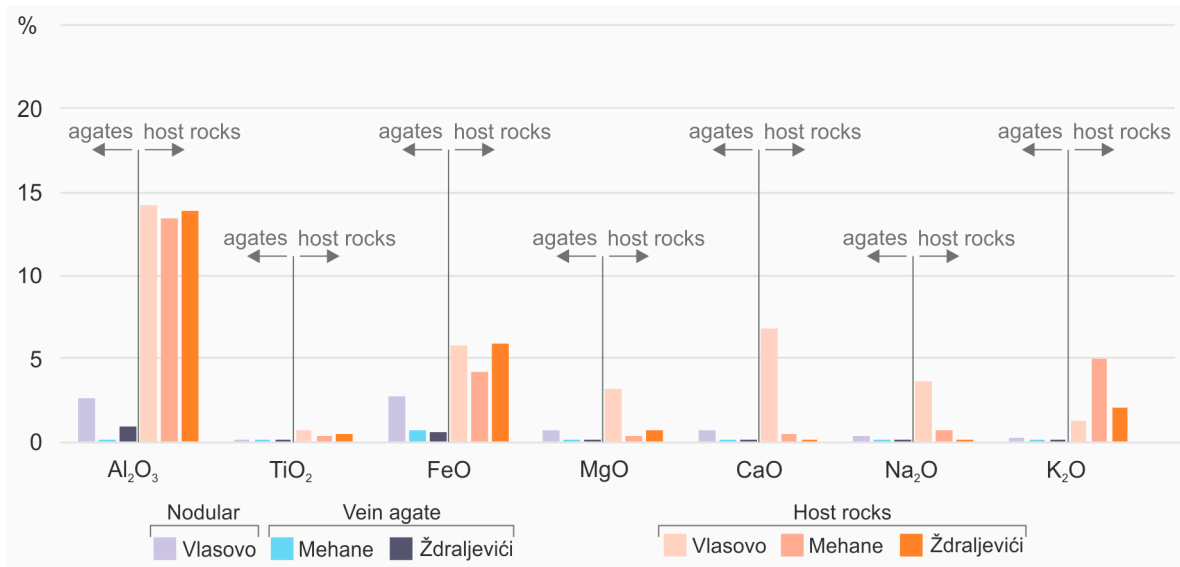
Figure 12. Comparison of major elements in agates and their host rocks from three agate occurrences of the Lece Volcanic Complex.

6. Discussion

The predominant host rocks of the agate occurrences are andesites with varying degrees of hydrothermal alteration. The vein agate host rocks at Rasovača, Ždraljevići, and Mehane occurrences demonstrate intense hydrothermal alteration. The high degree of silicification at these locations has led to a reduced weight percentage of major elements of the host rocks (Table 2, Figure 12). The effects of intense hydrothermal activity are also evident in the enrichment of the host rocks with metallic ore elements, especially Pb in the Ždraljevići agate host rock. Nodular agate host rocks (Vlasovo) are less altered with the weight percentage of the major compounds remaining mostly undisturbed (Table 2).

The agates found at Rasovača, Mehane, and Ždraljevići occur in the form of veins, with Rasovača exhibiting the most intense brecciation. However, brecciation is also observed in parts of the agate veins at the Ždraljevići and Mehane locations. In contrast, the Vlasovo and Sokolov Vis agates occur in the nodular form.

Silica phases of the agates from the Lece Volcanic Complex comprise opal-CT, length-fast chalcedony, quartzine, microcrystalline and macrocrystalline quartz. Length-fast chalcedony exhibits a helical twisting of fibers along the c-axis (also known as "runzelbanderung" [51,52]), forming what is known as zebraic chalcedony.

The presence of silica phases varies among the agate occurrences. At the Rasovača and Mehane vein agate occurrences, chalcedony and quartz are equally represented, forming separate agate bands. In the Ždraljevići agates, quartz is the most abundant silica phase. Opal-CT is absent from all vein agate occurrences. In the nodular agate occurrences of Vlasovo and Sokolov Vis, chalcedony is the most represented silica phase, alongside the presence of opal-CT and macrocrystalline quartz.

The presence of Bambauer quartz (Figure 4E) in vein agates indicates its formation in hydrothermal fluids characterized by fluctuations of silica concentrations and pH conditions [6,28,53–56]. It is supposed that these fluctuations in physicochemical conditions of hydrothermal fluids are responsible for the frequent alterations of different silica phases [53] in vein agates, especially in the Mehane and Rasovača agate occurrences.

The microtexture of jigsaw puzzle quartz, present in the veined agates of Mehane and Rasovača, supports the hypothesis of recrystallization of silica, previously deposited in the form of opal or chalcedony [6,57–59]. In these vein occurrences, silica was most likely originally deposited in the form of chalcedony, surrounding the jigsaw puzzle quartz (Figure 12). It is speculated that the jigsaw quartz was formed during the process

of recrystallization of amorphous or cryptocrystalline silica at temperatures exceeding 180 °C [55,57,60].

In the vein agates of Rasovača, Mehane, and Ždraljevići, a variety of textures, such as crustiform, colloform, comb, mosaic, flamboyant, and pseudobladed, are observed. All these primary, recrystallization, and replacement microtextures clearly indicate their formation in epithermal conditions of hydrothermal fluids [58]. Conversely, there is no such abundance of silica textures in the Lece nodular agates.

Quartzine occurs sporadically in the agates of the Lece Volcanic Complex. It is best represented in the Rasovača vein agate where it appears between quartz layers. Folk and Pittman [61] suggested a possible connection between the appearance of quartzine and sulphate-rich solutions or evaporitic conditions. However, these mechanisms and conditions of depositions of length-slow chalcedony have not been fully and conclusively explained to date [3,62].

Opal-CT found in nodular agate samples is generally characterized by low water content, inferred from the observed weak intensity of bands in the OH-region. Conversely, vein agate samples do not show any features in the OH-region, suggesting that they are virtually anhydrous. The absence of opal-CT in vein agates indicates a higher degree of silica crystallinity. Part of the silica probably crystallized directly from hydrothermal solutions. The presence of zoned quartz crystals, especially in the Rasovača and Ždraljevići agates, supports the hypothesis of direct crystallization [3]. In contrast, opal-CT in nodular agates indicates that silica phases crystallized from amorphous precursors, with opal representing the intermediate stage between amorphous and crystalline silica [3,63–65].

Geochemical (ICP-MS) analyses revealed elevated concentrations of some ore elements (Table 2, Figure 11B), underscoring the significant role of hydrothermal ore solutions in the creation of the vein agate occurrences of the Mehane and Ždraljevići. Hydrothermal fluids circulating along fracture zones also contributed to the enrichment of ore elements in agate host rocks, particularly in the Ždraljevići occurrence. In contrast, the Vlasovo nodular agate has higher concentrations of major elements (Table 2, Figure 12) compared to the vein agates of Mehane and Ždraljevići. The creation of nodular agate can potentially be linked to later stages of hydrothermal activity occurring in the near-surface conditions. Moreover, the chemical composition of hydrothermal fluids was probably different from those causing the formation of vein agates in the fracture zone domain. The hydrothermal fluids responsible for the formation of nodular agates probably caused the leaching of andesitic rocks, resulting in elevated contents of major elements in the Vlasovo nodular agate compared to vein agates (Table 2, Figures 11 and 12).

ICP-MS analyses reveal elevated Ba concentrations in the Mehane agate specimens, thus confirming the presumed presence of barite, supported by optical microscopy, XRD, and FTIR analyses. Due to the high solubility of sulfate minerals, barite could be easily dissolved during prolonged hydrothermal activity, which would result in pseudomorphism of quartz after barite. As it is a very frequent mineral in hydrothermal deposits, barite also confirms the hydrothermal origin of vein agates of the Lece Volcanic Complex. While calcite often accompanies barite in vein agates, it has not been proven by the results of either of the analytical methods implemented in this study. However, the presence of calcite should not be completely ruled out, since some textural features in vein agates, especially in the Mehane and Rasovača agates, indicate its possible presence overridden by the abundant influx of silica minerals.

Iron oxides are common paragenetic minerals in agates [3,55]. Based on the results of ICP-MS, SEM, XRD, and FTIR analyses, iron oxides are found in both the vein and nodular agates of the Lece Volcanic Complex. Two iron oxide and hydroxide minerals were identified: hematite and goethite.

Iron oxide minerals can be found both in the contact zone between volcanic host rock and agate and in the agate matrix. They form variously shaped individual inclusions with occasional accumulations (Figure 5A,B and 6A). Additionally, iron oxides appear as fine crystalline inclusions along agate bands (Figure 5C). These iron oxide inclusions

contribute to the coloration of particular bands of both vein and nodular agates (Figure 3). Iron oxides in nodular agate most likely originate from volcanic host rocks, released during alteration processes. Based on a laboratory experimental investigation, the crystallization of hematite and goethite varies with pH levels, in conditions of low pressure and temperatures between 100 and 200 °C [66,67]. The presence of hematite and goethite implies strong pH fluctuations between acidic and alkaline conditions during agate formation [68].

Based on the findings of FTIR analysis, organic matter is found in both vein and nodular agates, but they are probably of a different origin. The presence of filamentous forms in the nodular agates (Figure 3H) indicates its formation in near-surface conditions [69–71]. Those filamentous forms could potentially be products of microbial activity in near-surface cavities in andesitic volcanic rocks of the Lece Volcanic Complex. According to Götze et al. [71], such biological activity implies maximum temperatures of 100–120 °C and near-neutral pH conditions. In contrast, organic matter in the vein agates was probably incorporated in the hydrothermal solutions from deep-laying or surrounding lithological units. However, it is also possible that organic matter was deposited in the vein agates due to the mixing of organic matter carrying meteoric water and ascending hydrothermal solutions. The high aliphatic component observed in the FTIR spectra of vein agates is significant in that respect.

Placer agate varieties are similar to those found in primary occurrences, yet with some completely new and different textural varieties (Figure 3M–O). Based on this, the geological potential of the Lece Volcanic Complex is expected to be far greater with regard to agate than the current level of explorations has revealed. Thus, we can anticipate that future discoveries will encompass not only new agate occurrences, but also new textural varieties.

The findings of this study highlight the diversity in the genesis of agate occurrences in the Lece Volcanic Complex. Three agate occurrences (Rasovača, Mehane, and Ždraljevići) are related to fracture zones. Faults within previously formed volcanic rocks were generated due to the tectonic movements of the final phases of volcanic activity, which also enabled the formation of hydrothermal systems. The hydrothermal solutions were likely enriched with silica coming from different lithological units and from previously formed volcanic rocks. Silica transported in hot fluids was deposited along fault zones due to altered equilibrium conditions, such as a decreased pressure and temperature, pH change, silica oversaturation, etc. [3,57]. The intense brecciation of both volcanic rocks and agate highlights multiphase hydrothermal and tectonic activity. Increased contents of metallic ore elements in the vein agates indicate their genetic connection with polymetallic hydrothermal ore deposits of the Lece Volcanic complex, which is a part of the Lece-Chalkidiki metallogenic zone [72,73].

The nodular agates from the Vlasovo and Sokolov Vis sites appear to have formed under distinct conditions. Their mineralization is not related to fracture zones. Agates are formed within small voids located in the upper portions of volcanic bodies. Silica probably originated from andesitic volcanic rocks altered under the influence of hot surface fluids. It may have been transported by diffusion through porous volcanic rocks [55,74,75]. Another possible source of silica is the silica-rich thermal springs that formed siliceous sinters widely distributed throughout the Lece Volcanic Complex.

7. Conclusions

This paper provides the initial findings of geological, mineralogical, and geochemical investigations of agates from andesites within the Oligocene-Miocene Lece Volcanic Complex (Serbia).

Five primary vein and nodular agate occurrences have been discovered in the andesites of the Lece Volcanic Complex. Significant differences between the agate occurrences have been established regarding their mode of occurrence, macroscopic features, mineral composition, microtextural features, and geochemical characteristics.

The mineral composition of vein agates is primarily characterized by the presence of chalcedony and quartz. Chalcedony is typically length-fast, with quartzine occurring sporadically. Within the Ždraljevići vein agate, macroquartz emerges as the predominant

silica phase. Opal-CT is absent in vein agates, while barite and Fe-oxides represent the main mineral inclusions. Nodular agate, on the other hand, predominantly comprises length-fast chalcedony, alongside the presence of opal-CT and macrocrystalline quartz. Iron oxides are also widely present mineral inclusions in nodular agates.

Agates at the Rasovača, Ždraljevići, and Mehane, which are related to fracture zones, form vein-type occurrences. Their origin is epithermal hydrothermal associated with the polymetallic ore deposits of the Lece Volcanic Complex.

In the remaining two primary occurrences, Vlasovo and Sokolov Vis, silica fills the cavities in andesites forming volcanic (nodular) agates. These occurrences are spatially unrelated to the hydrothermal vein agate occurrences. The cavities in andesites are filled with silica that presumably originated from volcanic lithologies weathered by surficial hydrothermal hot fluids [55,75]. Filamentous forms in the Vlasovo agate, which indicate microbial activity, further support a near-surface agate formation [69–71].

The significant geological potential of the Lece Volcanic complex, regarding agate occurrences, is further confirmed with the secondary alluvial placers where agate varieties still unknown in the primary occurrences have been discovered.

References

1. Graetsch, H. Structural characteristics of opaline and microcrystalline silica minerals. *Rev. Mineral. Geochem.* **1994**, *29*, 209–232.
2. Moxon, T. *Studies of Agate*; Terra Publications: Doncaster, UK, 2009; 96p.
3. Götze, J. *Agate-Fascination between Legend and Science*; Agates Zenz, J., III, Ed.; Bode-Verlag: Salzhemmendorf, Germany, 2011; pp. 19–133.
4. Moxon, T.; Reed, S.J.B. Agate and chalcedony from igneous and sedimentary hosts aged from 13 to 3480 Ma: A cathodoluminescence study. *Mineral. Mag.* **2006**, *70*, 485–498. [CrossRef]
5. Götte, J.; Möckel, R.; Kempe, U.; Kapitonov, I.; Vennemann, T. Characteristics and origin of agates in sedimentary rocks from the Dryhead area, Montana. USA. *Mineral. Mag.* **2009**, *73*, 673–690. [CrossRef]
6. Pršek, J.; Dumanska-Słowik, M.; Powolny, T.; Natkaniec-Nowak, L.; Toboła, T.; Zych, D.; Skrepnicka, D. Agates from Western Atlas (Morocco)—Constraints from mineralogical and microtextural characteristics. *Minerals* **2020**, *10*, 198. [CrossRef]
7. Götze, J.; Möckel, R.; Vennemann, T.; Müller, A. Origin and geochemistry of agates in Permian volcanic rocks of the Sub-Erzgebirge basin, Saxony (Germany). *Chem. Geol.* **2016**, *428*, 77–91. [CrossRef]
8. Ilić, M.; Malešević, N.; Pejčić, M.; Miladinović, Z. A review of gem raw materials of Serbia. *Vesn. Geozavoda* **1998**, *48*, 169–201. (In Serbian)
9. Antonović, A. Agate occurrences on Fruška Gora Mt. *Zapisnici Srp. Geološkog Društva 1980 God.* **1981**, 21–24. (In Serbian)
10. Ilić, M.; Tošović, R.; Miladinović, Z.; Antonović, A. Gem raw materials of the Frushka Gora mountain (Serbia): Geological characteristics and economic significance of deposits. In Proceedings of the XVIIth Congress of Carpathian-Balkan Geological Association, Bratislava, Slovakia, 1–4 September 2002.
11. Miladinović, Z. Hopovo gemstone occurrence (Fruška Gora). *Teh.—Min. Geol. Metall.* **2020**, *71*, 305–312. [CrossRef]
12. Ilić, M.; Miladinović, Z.; Simić, V. A contribution to the knowledge of the gem mineral deposit Boblija near Gornji Milanovac. In Proceedings of the VIIth International Conference Nemetali, Banja Vrujci, Serbia, 25–28 October 2006. (In Serbian)
13. Miladinović, Z.; Simić, V.; Jelenković, R.; Ilić, M. Gemstone deposits of Serbia. *Geol. Carpathica* **2016**, *67*, 211–222. [CrossRef]
14. Marčeta, L. Geological Characteristics of Gemstone Occurrences in Šumadija District. Master's Thesis, Faculty of Mining and Geology, University of Belgrade, Belgrade, Serbia, 2005; 109p. (In Serbian)

15. Miladinović, Z.; Ilić, M.; Simić, V. Gemstone deposits of Lece Volcanic Complex (South Serbia). In Proceedings of the XIXth Congress of Carpathian-Balkan Geological Association, Thessaloniki, Greece, 23–26 September 2010; Geologica Balcanica: Sofia, Bulgaria, 2010; Volume 39, pp. 253–254.

16. Cissarz, A.; Pešut, D. *Izveštaj o Istražnim Radovima Poludragog Kamena u Okolini Rudnika Lece*; FSD Geozavoda: Beograd, Serbia, 1953. (In Serbian)

17. Miladinović, Z. Mineragenetic Characteristics and Potentiality of Gem Mineral Resources of the Lece Volcanic Complex. Ph.D. Thesis, Faculty of Mining and Geology, University of Belgrade, Belgrade, Serbia, 2012; 211p. (In Serbian). Available online: https://nardus.mpn.gov.rs/handle/123456789/6291 (accessed on 15 April 2024).

18. Malešević, M.; Vukanović, M.; Brković, T.; Obradinović, Z.; Karajčić, Z.; Stanisavljević, R.; Dimitrijević, M.; Urošević, M. *Basic Geological Map of SFR Yugoslavia, 1:100.000, Sheet Kuršumlija*; Savezni geološki zavod: Belgrade, Serbia, 1979. (In Serbian)

19. Rakić, M.; Dimitrijević, M.D.; Terzin, V.; Cvetković, D.; Petrović, V. *Basic Geological Map of SFR Yugoslavia, 1:100.000, Sheet Niš*; Savezni geološki zavod: Belgrade, Serbia, 1973. (In Serbian)

20. Vukanović, M.; Karajičić, L.; Dimitrijević, M.; Možina, A.; Gagić, A.; Jevremović, M. *Basic Geological Map of SFR Yugoslavia, 1:100.000, Sheet Leskovac*; Savezni geološki zavod: Belgrade, Serbia, 1969. (In Serbian)

21. Vukanović, M.; Dimitrijević, M.D.; Dimitrijević, M.N.; Karajičić, L.; Rajčević, D.; Navala, M.; Urošević, M.; Malešević, M.; Trifunović, S.; Serdar, R.; et al. *Basic Geological Map of SFR Yugoslavia, 1:100.000, Sheet Podujevo*; Savezni geološki zavod: Belgrade, Serbia, 1982. (In Serbian)

22. Pešut, D. Geološki Sastav, Tektonska Struktura i Metalogenija Leckog Masiva. Ph.D. Thesis, Faculty of Mining and Geology, University of Belgrade, Belgrade, Serbia, 1961. (In Serbian)

23. Pešut, D. *Geološki Sastav, Tektonska Struktura i Metalogenija Leckog Masiva. Geology, Tectonics and Metallogeny of Lece Massif*; Rasprava XIV, Vol. XIV; Rasprave Zavoda za Geološka i Geofizička Istraživanja, Memoires du Service Geologique et Geofisique: Belgrade, Serbia, 1976; Volume 59. (In Serbian)

24. Serafimovski, T. *Structural-Metallogenetic Characteristics of Lece-Chalkidiki Zone: Types of Deposits and Reionization*; Faculty of Mining and Geology: Štip, North Macedonia, 1993; 328p, (In North Macedonian Language).

25. Kostić, B.; Cvetković, V.; Šarić, K.; Krstekanjić, N.; Pantelić, N.; Bosić, D. A reinterpretation of the geological map of the northwestern part of the Lece Volcanic Complex. In *EGU Series: Émile Argand Conference, Proceedings of the 13th Workshop on Alpine Geological Studies, Belgrade, Serbia, 7–18 September 2017*; University of Belgrade Faculty of Mining and Geology: Belgrade, Serbia, 2017; p. 55.

26. Miladinović, Z. Alluvial placer gemstone occurrence of The Velika Kosanica river (Lece Volcanic Complex). In Proceedings of the XVIII Serbian Geological Congress, Divčibare, Serbia, 1–4 June 2022; pp. 169–170.

27. Menges, F. Spectragryph—Optical Spectroscopy Software, Version 1.2.16.1. 2022. Available online: https://www.effemm2.de/spectragryph/ (accessed on 15 April 2024).

28. Bambauer, H.U.; Brunner, G.O.; Laves, F. Beobachtungen über Lamellen bau an Bergkristallen. *Z. Krist.* **1961**, *116*, 173–181. (In German) [CrossRef]

29. Jones, J.B.; Segnit, E.R. The nature of opal I. Nomenclature and constituent phases. *J. Geol. Soc. Aust.* **1971**, *18*, 57–68. [CrossRef]

30. Ghisoli, C.; Caucia, F.; Marinoni, L. XRPD patterns of opals: A brief review and new results from recent studies. *Powder Diffr.* **2010**, *25*, 274–282. [CrossRef]

31. Flörke, O.W. Zur Frage des "Hoch"-Cristobalit in Opalen, Bentoniten und Gläsern. *Neues Jahrb. Mineral. Monatshefte* **1955**, *10*, 217–224.

32. Smith, D.K. Opal, cristobalite, and tridymite: Noncrystallinity versus crystallinity, nomenclature of the silica minerals and bibliography. *Powder Diffr.* **1998**, *13*, 2–19. [CrossRef]

33. Wilson, M.J. The structure of opal-CT revisited. *J. Non-Cryst. Solids* **2014**, *405*, 68–75. [CrossRef]

34. McDonald, R.S. Surface Functionality of Amorphous Silica by Infrared Spectroscopy. *J. Phys. Chem.* **1958**, *62*, 1168–1178. [CrossRef]

35. Mori, T.; Kuroda, Y.; Yoshikawa, Y.; Nagao, M.; Kittaka, S. Preparation of a Water-Resistant Siliceous MCM-41 Sample, through Improvement of Crystallinity, and Its Prominent Adsorption Features. *Langmuir* **2002**, *18*, 1595–1603. [CrossRef]

36. Paukshtis, E.A.; Yaranova, M.A.; Batueva, I.S.; Bal'Zhinimaev, B.S. A FTIR study of silanol nests over mesoporous silicate materials. *Microporous Mesoporous Mater.* **2019**, *288*, 109582. [CrossRef]

37. Lin-Vien, D.; Colthup, N.B.; Fateley, W.G.; Grasselli, J.G. *The Handbook of Infrared and Raman Characteristic Frequencies of Organic Molecules*; Academic Press: Boston, MA, USA, 1991; Volume xvi, p. 503.

38. Popescu, C.-M.; Jones, D.; Kržišnik, D.; Humar, M. Determination of the effectiveness of a combined thermal/chemical wood modification by the use of FT-IR spectroscopy and chemometric methods. *J. Mol. Struct.* **2020**, *1200*, 127133. [CrossRef]

39. Ibarra, J.; Muñoz, E.; Moliner, R. FTIR study of the evolution of coal structure during the coalification process. *Org. Geochem.* **1996**, *24*, 725–735. [CrossRef]

40. Yin, Y.; Yin, H.; Wu, Z.; Qi, C.; Tian, H.; Zhang, W.; Hu, Z.; Feng, L. Characterization of Coals and Coal Ashes with High Si Content Using Combined Second-Derivative Infrared Spectroscopy and Raman Spectroscopy. *Crystals* **2019**, *9*, 513. [CrossRef]

41. Liang, C.Y.; Marchessault, R.H. Infrared spectra of crystalline polysaccharides. II. Native celluloses in the region from 640 to 1700 cm^{-1}. *J. Polym. Sci.* **1959**, *39*, 269–278. [CrossRef]

42. Kacuráková, M.; Smith, A.; Gidley, M.; Wilson, R. Molecular interaction in bacterial cellulose composites studied by 1D FT-IR and dynamic 2D FTIR spectroscopy. *Carbohydr. Res.* **2002**, *337*, 1145–1153. [CrossRef] [PubMed]

43. Garside, P.; Wyeth, P. Identification of Cellulosic Fibres by FTIR Spectroscopy I: Thread and Single Fibre Analysis by Attenuated Total Reflectance. *Stud. Conserv.* **2003**, *48*, 269–275. [CrossRef]

44. Boeriu, C.G.; Bravo, D.; Gosselink, R.J.; van Dam, J.E. Characterisation of structure-dependent functional properties of lignin with infrared spectroscopy. *Ind. Crop. Prod.* **2004**, *20*, 205–218. [CrossRef]

45. Adler, H.H.; Kerr, P.F. Variations in infrared spectra, molecular symmetry and site symmetry of sulfate minerals. *Am. Mineral.* **1965**, *50*, 132–147.

46. Shen, Y.; Li, C.; Zhu, X.; Xie, A.; Qiu, L.; Zhu, J. Study on the preparation and formation mechanism of barium sulphate nanoparticles modified by different organic acids. *J. Chem. Sci.* **2007**, *119*, 319–324. [CrossRef]

47. Veneranda, M.; Aramendia, J.; Bellot-Gurlet, L.; Colomban, P.; Castro, K.; Madariaga, J.M. FTIR spectroscopic semi-quantification of iron phases: A new method to evaluate the protection ability index (PAI) of archaeological artefacts corrosion systems. *Corros. Sci.* **2018**, *133*, 68–77. [CrossRef]

48. Kaufhold, S.; Ufer, K.; Hein, M.; Götze, N.; Dohrmann, R. A combined IR and XRD study of natural well crystalline goethites (α-FeOOH). *Acta Geochim.* **2022**, *41*, 794–810. [CrossRef]

49. Chukanov, N.V. *Infrared Spectra of Mineral Species, Extended Library*; Springer Geochemistry/Mineralogy; Springer International Publishing: Dordrecht, The Netherlands, 2014; Volume 1, p. 1726.

50. Condie, K.C. Chemical composition and evolution of the upper continental crust: Contrasting results from surface samples and shales. *Chem. Geol.* **1993**, *104*, 1–37. [CrossRef]

51. Wang, Y.; Merino, E. Self-organisational origin of agates: Banding fiber twisting, composition and dynamic crystallization model. *Geochim. Cosmochim. Acta* **1990**, *54*, 1627–1638. [CrossRef]

52. Heany, P.J. A proposed mechanism for the growth of chalcedony. *Contrib. Mineral. Petrol.* **1993**, *115*, 66–74. [CrossRef]

53. Richter, S.; Götze, J.; Niemeyer, H.; Möckel, R. Mineralogical investigation of agates from Cordón de Lila, Chile. *J. Andean Geol.* **2015**, *42*, 386–396.

54. Powolny, T.; Dumanska-Słowik, M.; Sikorska-Jaworowska, M.; Wójcik-Bania, M. Agate mineralization in spilitized Permian volcanics from "Borówno" quarry (Lower Silesia, Poland)—Microtextural, mineralogical, and geochemical constraints. *Ore Geol. Rev.* **2019**, *114*, 103–130. [CrossRef]

55. Götze, J.; Möckel, R.; Pan, Y. Mineralogy, Geochemistry and Genesis of Agate—A Review. *Minerals* **2020**, *10*, 1037. [CrossRef]

56. Conte, A.; Della Ventura, G.; Rondeau, B.; Romani, M.; Guidi, M.C.; La, C.; Napoleoni, C.; Lucci, F. Hydrothermal genesis and growth of the banded agates from the Allumiere-Tolfa volcanic district (Latium, Italy). *Phys. Chem. Miner.* **2022**, *49*, 39. [CrossRef]

57. Fournier, R.O. The behavior of silica in hydrothermal solutions. *Rev. Econ. Geol.* **1985**, *2*, 45–60.

58. Dong, G.; Morrison, G.; Jaireth, S. Quartz textures in epithermal veins, Queensland—Classification, origin, and implication. *Econ. Geol.* **1995**, *90*, 1841–1856. [CrossRef]

59. Yilmaz, T.I.; Duschl, F.; Di Genova, D. Feathery and network-like filamentous textures as indicators for the re-crystallization of quartz from a metastable silica precursor at the Rusey Fault Zone, Cornwall, UK. *Solid Earth* **2016**, *6*, 1509–1536. [CrossRef]

60. Saunders, J.A. Silica and gold textures in bonanza ores of the Sleeper deposit, Humboldt County, Nevada.: Evidence for colloids and implications for epithermal ore-forming processes. *Econ. Geol.* **1994**, *89*, 628–638. [CrossRef]

61. Folk, R.L.; Pittman, J.S. Length-slow chalcedony; A new testament for vanished evaporates. *J. Sediment. Petrol.* **1971**, *41*, 1045–1058.

62. Keene, J.B. Chalcedonic quartz and occurrence of quartzine (length-slow chalcedony) in pelagic sediments. *Sedimentology* **1983**, *30*, 449–454. [CrossRef]

63. Götze, J.; Nasdala, L.; Kleeberg, R.; Wenzel, M. Occurrence and distribution of "moganite" in agate/chalcedony: A combined micro-Raman, Rietveld, and cathodoluminescence study. *Contrib. Mineral. Petrol.* **1998**, *133*, 96–105. [CrossRef]

64. Moxon, T.; Ríos, S. Moganite and water content as a function of age in agate: An XRD and thermogravimetric study. *Eur. J. Mineral.* **2004**, *16*, 269–278. [CrossRef]

65. Liesegang, M.; Mielke, R.; Berthold, C. Amorphous silica maturation in chemically weathered clastic sediments. *Sediment. Geol.* **2018**, *365*, 54–61. [CrossRef]

66. Christensen, A.N. Hydrothermal preparation of goethite and haematite from amorphous iron (III) hydroxide. *Acta Chem. Scand.* **1968**, *22*, 1487–1490. [CrossRef]

67. Das, S.; Hendry, M.J.; Essilfie-Dughan, J. Transformation of Two-Line Ferrihydrite to Goethite and Hematite as a Function of pH and Temperature. Environ. *Sci. Technol.* **2011**, *45*, 268–275. [CrossRef] [PubMed]

68. Zhang, X.; Ji, L.; He, X. Gemological characteristics and origin of the Zhanguohong agate from Beipiao, Liaoning province, China: A combined microscopic, X-ray diffraction, and Raman spectroscopic study. *Minerals* **2020**, *10*, 401. [CrossRef]

69. Hofmann, B.; Farmer, J. Filamentous fabrics in low-temperature mineral assemblages: Are they fossil biomarkers? Implications for the search for a subsurface fossil record on the early Earth and Mars. *Planet. Space Sci.* **2000**, *48*, 1077–1086. [CrossRef]

70. Johannessen, K.C.; McLoughlin, N.; Vullum, P.E.; Thorseth, I.H. On the biogenicity of Fe-oxyhydroxide filaments in silicified low-temperature hydrothermal deposits: Implications for the identification of Fe-oxidizing bacteria in the rock record. *Geobiology* **2019**, *18*, 31–53. [CrossRef]

71. Götze, J.; Hofmann, B.; Machałowski, T.; Tsurkan, M.V.; Jesionowski, T.; Ehrlich, H.; Kleeberg, R.; Ottens, B. Biosignatures in Subsurface Filamentous Fabrics (SFF) from the Deccan Volcanic Province, India. *Minerals* **2020**, *10*, 540. [CrossRef]

72. Jelenkovic, R.; Kostić, A.; Životić, D.; Ercegovac, M. Mineral resources of Serbia. *Geol. Carpathica* **2008**, *59*, 345–361.
73. Serafimovski, T. The Lece-Chalkidiki metallogenic zone: Geotectonic setting and metallogenic features. *Geologija* **1999**, *42*, 159–164. [CrossRef]
74. Götze, J.; Schrön, W.; Möckel, R.; Heide, K. The role of fluids in the formation of agates. *Chem. Erde—Geochem.* **2012**, *72*, 283–286. [CrossRef]
75. Moxon, T.; Palyanova, G. Agate Genesis: A Continuing Enigma. *Minerals* **2020**, *10*, 953. [CrossRef]